

Multi-band analysis on physical properties of superconducting FeSe films

Jian-Tao Che(车剑韬) and Chen-Xiao Ye(叶晨骁)

Citation: Chin. Phys. B, 2023, 32 (**9**): 097401. DOI: 10.1088/1674-1056/acd3e5
Journal homepage: http://cpb.iphy.ac.cn; http://iopscience.iop.org/cpb

What follows is a list of articles you may be interested in

Anisotropic superconducting properties of $FeSe_{0.5}Te_{0.5}$ single crystals

Jia-Ming Zhao(赵佳铭) and Zhi-He Wang(王智河)
Chin. Phys. B, 2022, 31 (**9**): 097402. DOI: 10.1088/1674-1056/ac5610

Phase-field simulation of superconductor vortex clustering in the vicinity of ferromagnetic domain bifurcations

Hasnain Mehdi Jafri, Jing Wang(王静), Chao Yang(杨超), Jun-Sheng Wang(王俊升), and Hou-Bing Huang(黄厚兵)
Chin. Phys. B, 2020, 29 (**12**): 127402. DOI: 10.1088/1674-1056/abb22c

Generalized Drude model and electromagnetic screening in metals and superconductors

Da Wang(王达)
Chin. Phys. B, 2018, 27 (**5**): 057401. DOI: 10.1088/1674-1056/27/5/057401

Fluctuating specific heat in two-band superconductors

Lei Qiao(乔雷), Cheng Chi(迟诚), Jiangfan Wang(王江帆)
Chin. Phys. B, 2017, 26 (**11**): 117401. DOI: 10.1088/1674-1056/26/11/117401

Multi-band analysis on physical properties of superconducting FeSe films

Jian-Tao Che(车剑韬)[1,†] and Chen-Xiao Ye(叶晨骁)[2]

[1] *Department of Mathematics and Physics, North China Electric Power University, Beijing* 102206, *China*
[2] *School of Nuclear Science and Engineering, North China Electric Power University, Beijing* 102206, *China*

(Received 10 November 2022; revised manuscript received 22 April 2023; accepted manuscript online 10 May 2023)

The origins of superconductivity and pairing symmetry of order parameters are still controversial problems for FeSe thin films up to date. Under the Neumann boundary conditions, the electromagnetic properties of this system are investigated using the two-band Ginzburg–Landau theory. We calculate the temperature dependence of upper critical field in arbitrary direction and critical supercurrent density through the FeSe film. It is revealed that the normalized upper critical field is independent of the film thickness and all of our theoretical results are in accordance with the experimental data. These thus strongly indicate the existence of two-gap s-wave superconductivity in this material.

Keywords: Ginzburg–Landau theory, two-band s-wave superconductivity, FeSe film

PACS: 74.20.De, 74.20.Rp, 74.78.−w **DOI:** 10.1088/1674-1056/acd3e5

1. Introduction

The discovery of iron-based materials with high superconducting transition temperatures has triggered great interest for both fundamental research and practical applications in this field.[1] Among these superconductors, the FeSe system has the simple crystal structure, clean superconducting phase, and low toxicity, thus making it an appealing candidate for studying the superconducting properties of iron-based compounds.[2] Although the superconducting transition temperature for bulk FeSe is relatively low ($T_c \sim 8$ K),[2,3] it can be significantly enhanced by applying high pressure,[4–6] intercalating alkali metal atoms like potassium[7–15] or most amazingly, by growing FeSe thin films on $SrTiO_3$ substrates with reported values of T_c up to 100 K.[16–18] Several approaches to the deposition of FeSe films such as pulsed laser deposition and molecular beam epitaxy techniques have been reported so far.[19–21] The FeSe layers consist of square lattices of Fe atoms with tetrahedrally coordinated covalent bonds to the Se anions, and the lattice constant perpendicular to the layered plane is about 0.55 nm.[22] This textured structure is suitable for research of low-dimensional electronic transport on substrates. For instance, Farrar *et al.* have observed signatures of the Berezinskii–Kosterlitz–Thouless transition for FeSe thin films and reported that a highly two-dimensional pairing channel dominates the superconductivity in this system.[23]

Recent studies on the electronic band structures have suggested that strong electron correlation plays a crucial role in understanding the physical properties of the FeSe compound. Based on dynamical mean field calculations, the existence of a lower Hubbard band is demonstrated for the electronic structure and this correlated electron system exhibits the non-Fermi liquid behavior due to the formation of local moments over an extended temperature range.[24] With soft-x-ray and hard-x-ray photoemission spectroscopy, the detection of the Fe 3d band narrowing and the energy shift of the band toward the Fermi level also indicate the importance of the electron correlation effect in FeSe.[25] Later, Jiang *et al.* pointed out that the Fe–Fe interatomic Coulomb repulsion actually offers a natural explanation for the emergent nematic order, the absence of magnetism, and at a more fundamental level, the unusually large band renormalization in the FeSe system.[26] Based on the extended Hubbard model, it has also been argued that the interatomic Coulomb interactions favor s-wave pairing[27] and will play an important role in stabilizing the s-wave pairing symmetry in Fe-based superconductors.[28]

To date, there have been several investigations on the pairing symmetry of the superconducting FeSe film. The experimental data of superfluid density for an ultrathin FeSe system can be fitted down to 10 K using the standard Bardeen–Cooper–Schrieffer (BCS) theory, which gives a gap of 10.1 meV at zero temperature and shows the nodeless structure in the excitation spectrum.[29] However, the unusual upturn of the superfluid density around 5 K may also point to the presence of a second (small) gap in this system. Meanwhile, the measurements from the scanning tunneling microscopy have reported the gap structure with double peaks at 2.3 meV and 1.5 meV for the superconducting state of the FeSe compound.[30] Moreover, the anisotropy of the upper critical fields decreases with the decreasing temperature and reveals a pseudoisotropic behavior in this process, which is also indicative of the multi-band character for this material.[31] The strong temperature dependence of Hall sensitivity for the

[†]Corresponding author. E-mail: chejt2013@163.com

© 2023 Chinese Physical Society and IOP Publishing Ltd

FeSe film shows the similar effect.[32] Thus, there is still no general consensus on the form of superconducting order parameter in the FeSe film to date, and further explorations to elucidate this issue are necessary.

The main purpose of this paper is to investigate the electromagnetic properties of the FeSe film using the two-band Ginzburg–Landau (GL) theory. We derive the two-band GL equations for the two-gap superconducting film, and then compute the temperature dependence of upper critical field in arbitrary direction and critical supercurrent density through this system. It is found that the normalized upper critical field $H_{c2}(T)/H_{c2}(0)$ is independent of the film thickness and all the results are in good agreement with the experimental data. These thus suggest that the FeSe film system is a two-gap s-wave superconductor. As a byproduct, our calculations also show that the ratio of the effective masses between these two bands is about 6.2.

The rest of this article is organized as follows. In Section 2, we introduce the two-band GL theory and apply this formalism to the quasi-two-dimensional superconductor. In Section 3, we compute the temperature and angular dependence of upper critical fields in the FeSe film. In Section 4, we calculate the temperature dependence of critical supercurrent density through the film. Finally, we conclude this article in Section 5.

2. The two-band Ginzburg–Landau theory

The GL free energy functional of two-gap superconductor with a small thickness d along the z (or c) direction can be written as[33–40]

$$F=\int_{-d/2}^{d/2}\left(f_1+f_2+f_{12}+\frac{\boldsymbol{H}^2}{8\pi}\right)\mathrm{d}z, \tag{1}$$

with

$$f_\gamma=\frac{\hbar^2}{2m_\gamma}\left|\left(\nabla-\frac{\mathrm{i}2e\boldsymbol{A}}{\hbar c}\right)\Delta_\gamma\right|^2-\alpha_\gamma(T)|\Delta_\gamma|^2+\frac{\beta_\gamma}{2}|\Delta_\gamma|^4, \tag{2}$$

$$f_{12}=-\varepsilon_{12}(\Delta_1^*\Delta_2+\mathrm{c.c.}), \tag{3}$$

where f_γ is the free energy density for band γ ($\gamma=1,2$), f_{12} is the interaction free energy density between these two bands, Δ_γ is the superconducting order parameter, m_γ represents the effective mass for band γ, and ε_{12} is the Josephson coupling constant. The coefficient α_γ is a function of temperature, while β_γ is independent of temperature. If the interband interaction is neglected, the GL functional can be reduced to two independent single-band problems with corresponding critical temperatures T_{c1} and T_{c2}, respectively. Thus, the coefficient α_γ can be approximately expressed as $\alpha_\gamma(T)=\alpha_{\gamma0}t_\gamma(T)=\alpha_{\gamma0}(1-T/T_{c\gamma})$, with $\alpha_{\gamma0}$ being the proportionality constant.[41] $\boldsymbol{H}=\nabla\times\boldsymbol{A}$ represents the magnetic field and $\boldsymbol{A}$ is the vector potential.

Actually the GL functional for the two-gap superconductor can be derived from the two-band BCS model, and the microscopic forms of all the parameters in the GL theory have been obtained in Ref. [35]. Without loss of generality, we can assume that T_{c1} corresponds to the band with the larger gap. With $\ln(T_{c1}/T)\approx t_1(T)$, we can expand the microscopic forms of α_1 and α_2 as linear functions of $t_1(T)$, and obtain the useful relation $\alpha_{10}/\alpha_{20}=T_{c1}/T_{c2}$. Since two gaps at low temperature appear at 2.3 and 1.5 meV, respectively,[30] we can roughly approximate T_{c1}/T_{c2} to $2.3/1.5\approx1.5$ from the BCS theory. Meanwhile, from the microscopic two-band BCS theory we can also obtain $\beta_1=\beta_2\equiv\beta$.[35] We notice that the GL free energy in Eqs. (1)–(3) is invariant under the scaling transformation: $\Delta_\gamma\to\sqrt{l}\Delta_\gamma$, $m_\gamma\to lm_\gamma$, $\alpha_\gamma\to\alpha_\gamma/l$, $\beta\to\beta/l^2$, $\varepsilon_{12}\to\varepsilon_{12}/l$ with l being the scaling factor. Thus for simplicity, we can set $m_2=m_e$ with m_e the electron mass.

For a smooth nonmagnetic insulator-superconductor or vacuum-superconductor interface, we assume that there is no current flowing through the boundary and the Neumann boundary condition can be applied on the macroscopic scale. Thus, the boundary conditions on both surfaces of the thin film are given by $\frac{\mathrm{d}\Delta_\gamma}{\mathrm{d}z}\big|_{z=\pm d/2}=0$. It is easy to see that if we approximate the order parameter Δ_γ to a constant along the z-axis, the Neumann boundary condition will be automatically satisfied.

3. The upper critical field

Now let us solve the problem of the nucleation of superconductivity in the presence of magnetic field $\boldsymbol{H}$. Without losing any generalization, we assume $\boldsymbol{H}=(H\sin\theta,0,H\cos\theta)$, where θ is the directional angle of the field from the z-axis. Then the vector potential can be chosen as $\boldsymbol{A}=(0,Hx\cos\theta-Hz\sin\theta,0)$. Noting that $\boldsymbol{A}$ is only related to x and z, we can write the solution in the form of $\Delta_\gamma(x,y,z)=\rho_\gamma(x,z)\mathrm{e}^{\mathrm{i}k_yy}$. Plugging this form into Eqs. (2) and (3), and neglecting the quartic terms in the free energy densities, we can rewrite f_γ and f_{12} as

$$\begin{aligned}f_\gamma=&\frac{\hbar^2}{2m_\gamma}\left(\frac{\partial\rho_\gamma}{\partial x}\right)^2+\frac{\hbar^2}{2m_\gamma}\left(\frac{\partial\rho_\gamma}{\partial z}\right)^2\\&+\left[\frac{2e^2(x\cos\theta-z\sin\theta)^2H^2}{m_\gamma c^2}-\frac{2e\hbar k_y(x\cos\theta-z\sin\theta)H}{m_\gamma c}\right.\\&\left.+\frac{\hbar^2k_y^2}{2m_\gamma}-\alpha_\gamma\right]\rho_\gamma^2,\end{aligned} \tag{4}$$

$$f_{12}=-2\varepsilon_{12}\rho_1\rho_2. \tag{5}$$

Meanwhile, the requirement of the Neumann boundary conditions demands that in the lowest order the wavefunction ρ_γ will have no z dependence, i.e., $\rho_\gamma(x,z)=\rho_\gamma(x)$. With this approximation, we then perform the integration on z in Eq. (1)

and obtain the total free energy as follows:

$$\frac{F}{d}=\sum_{\gamma}\left[\frac{\hbar^2}{2m_\gamma}\left(\frac{\mathrm{d}\rho_\gamma}{\mathrm{d}x}\right)^2+\frac{1}{2}m_\gamma\omega_\gamma^2(x-x_0)^2\rho_\gamma^2+\sigma_\gamma\rho_\gamma^2\right]-2\varepsilon_{12}\rho_1\rho_2+\frac{\boldsymbol{H}^2}{8\pi}. \tag{6}$$

Here we define

$$\omega_\gamma=\frac{2eH\cos\theta}{m_\gamma c},\quad x_0=\frac{\hbar ck_y}{2eH\cos\theta},\quad \sigma_\gamma=\frac{(edH\sin\theta)^2}{6m_\gamma c^2}-\alpha_\gamma. \tag{7}$$

By minimizing the free energy with ρ_γ in Eq. (6), the linearized two-band GL equations in the thin film can be written as

$$\left[-\frac{\hbar^2}{2m_1}\frac{\mathrm{d}^2}{\mathrm{d}x^2}+\frac{1}{2}m_1\omega_1^2(x-x_0)^2+\sigma_1\right]\rho_1-\varepsilon_{12}\rho_2=0, \tag{8}$$

$$\left[-\frac{\hbar^2}{2m_2}\frac{\mathrm{d}^2}{\mathrm{d}x^2}+\frac{1}{2}m_2\omega_2^2(x-x_0)^2+\sigma_2\right]\rho_2-\varepsilon_{12}\rho_1=0. \tag{9}$$

Obviously, the inclusion of the factor x_0 only shifts the location of the minimum of the effective potential, so it will be neglected hereafter.

In the absence of the magnetic field and close to the critical temperature, ρ_γ can be treated as constant, then Eqs. (8) and (9) are simplified to

$$\alpha_1\rho_1+\varepsilon_{12}\rho_2=0,\quad \alpha_2\rho_2+\varepsilon_{12}\rho_1=0. \tag{10}$$

From Eq. (10), we can obtain $\varepsilon_{12}^2=\alpha_1(T_\mathrm{c})\alpha_2(T_\mathrm{c})$, which will be used to determine ε_{12} in our calculations.

Now we try to work out the upper critical field of the FeSe film under the applied magnetic field. In the case of $\varepsilon_{12}=0$, we can obtain the solution to Eqs. (8) and (9) immediately by noting that, for each band, it is the Schrödinger equation for a particle bound in a harmonic oscillator potential. The resulting eigenvalues are $E_{\gamma,n}=(n+1/2)\hbar\omega_\gamma+\sigma_\gamma$ with n being a non-negative integer, and the ground wavefunctions corresponding to these two bands take the form of $(\nu_0/\pi)^{1/4}\mathrm{e}^{-\nu_0x^2/2}$, with $\nu_0=2\pi H/\Phi_0$ and the magnetic flux quantum $\Phi_0=\pi\hbar c/e$.

If $\varepsilon_{12}\neq0$, Eqs. (8) and (9) describe a system of the two coupled oscillators. To obtain the minimum eigenvalue of the coupled oscillators, we follow a variational approach. We propose the solution in the form of $\rho_\gamma=a_\gamma(\nu_0/\pi)^{1/4}\mathrm{e}^{-\nu_0x^2/2}$, where a_γ is constant. Thus for $n=0$, Eqs. (8) and (9) can be transformed to

$$\begin{aligned}\left(\frac{1}{2}\hbar\omega_1+\sigma_1\right)a_1-\varepsilon_{12}a_2=0,\\ \left(\frac{1}{2}\hbar\omega_2+\sigma_2\right)a_2-\varepsilon_{12}a_1=0.\end{aligned} \tag{11}$$

Then the upper critical field H_{c2} can be obtained from Eq. (11) as

$$\left(\frac{1}{2}\hbar\omega_1+\sigma_1\right)\left(\frac{1}{2}\hbar\omega_2+\sigma_2\right)=\varepsilon_{12}^2 \tag{12}$$

at $H=H_{\mathrm{c2}}$.

When $\theta=0^\circ$, from Eq. (12) we can obtain the exact expression of the upper critical field parallel to the z-direction as

$$H_{\mathrm{c2}}^{\parallel}(T)=\frac{\Phi_0}{2\pi\xi_0^2}\Big\{1.5\eta_m t_1(T)+t_2(T)+\sqrt{[1.5\eta_m t_1(T)-t_2(T)]^2+6\eta_m t_1(T_\mathrm{c})t_2(T_\mathrm{c})}\Big\}. \tag{13}$$

For $\theta=90^\circ$, we can obtain the upper critical field perpendicular to the z-direction as

$$H_{\mathrm{c2}}^{\perp}(T)=\sqrt{\frac{6\Phi_0H_{\mathrm{c2}}^{\parallel}(T)}{\pi d^2}}. \tag{14}$$

Here $\xi_0^2=\hbar^2/m_2\alpha_{20}$ and the effective mass anisotropy $\eta_m=m_1/m_2$.

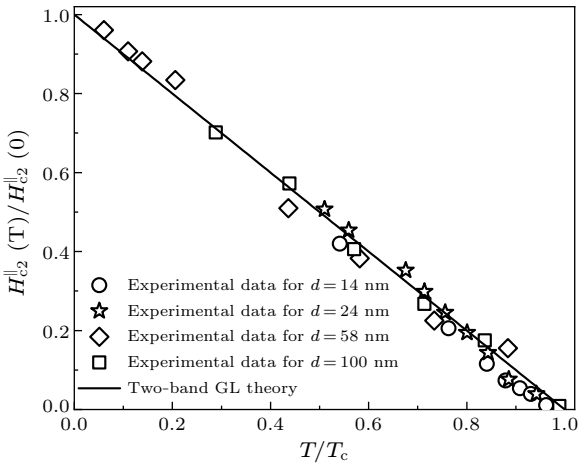


Fig. 1. The temperature dependence of normalized upper critical field parallel to the c-axis for the FeSe film thickness $d=14$ nm, 24 nm, 58 nm, and 100 nm. The experimental data are taken from Ref. [23].

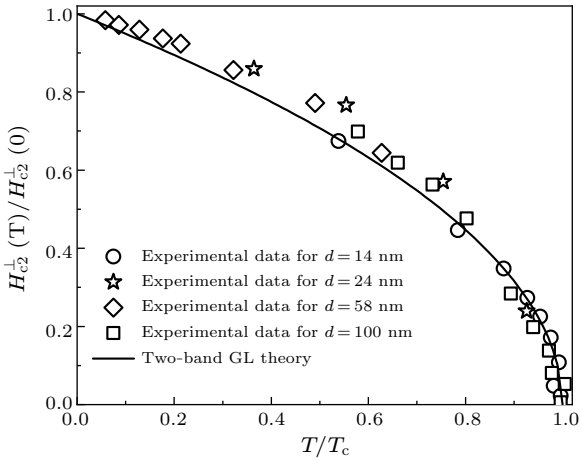


Fig. 2. Temperature dependence of normalized upper critical field perpendicular to the c-axis for the FeSe film. The experimental data of the FeSe films with the thickness $d=14$ nm, 24 nm, 58 nm and 100 nm are taken from Ref. [23].

We can easily obtain from Eqs. (13) and (14) that the normalized upper critical fields $H_{\mathrm{c2}}(T)/H_{\mathrm{c2}}(0)$ are independent of the film thickness d, and can be explicitly calculated

with two scale-invariant parameters η_m and $\eta_t = T_{c1}/T_c$. We choose $\eta_m = 6.2$ and $\eta_t = 0.93$ to fit the experimental data of the FeSe films. From Fig. 1, we can see that the data points of $H_{c2}^{\parallel}$ are almost linear in the whole temperature range below T_c and our calculations are consistent with the experimental measurements. Due to the simple relation between $H_{c2}^{\perp}$ and $H_{c2}^{\parallel}$ in Eq. (14), our theoretical results of $H_{c2}^{\perp}$ show the parabolic behavior and also well fit the experimental data with various film thicknesses in Fig. 2.

Furthermore, we can also perform the numerical computations on the angular dependence of the upper critical field according to Eq. (12). By taking one more parameter $\xi_0 = 0.36$ μm, we plot our results at $T = 2$ K for the 14 nm-thick FeSe film in Fig. 3. From Fig. 3, we can see that the upper critical field H_{c2} increases monotonously with the angle θ and our numerical calculations are consistent with the experimental data.

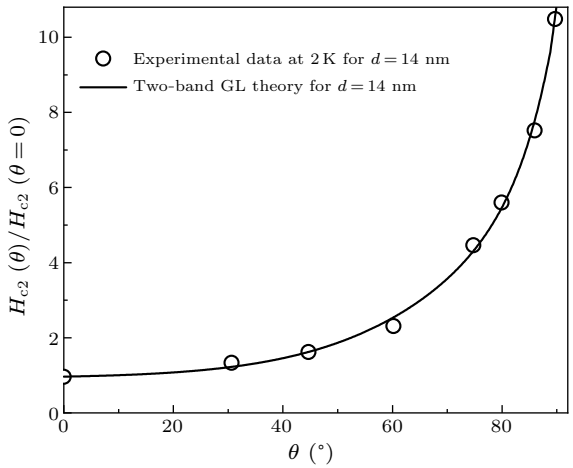


Fig. 3. Angular dependence of upper critical field at $T = 2$ K for the FeSe film. The experimental data of FeSe with the thickness $d = 14$ nm are taken from Ref. [23].

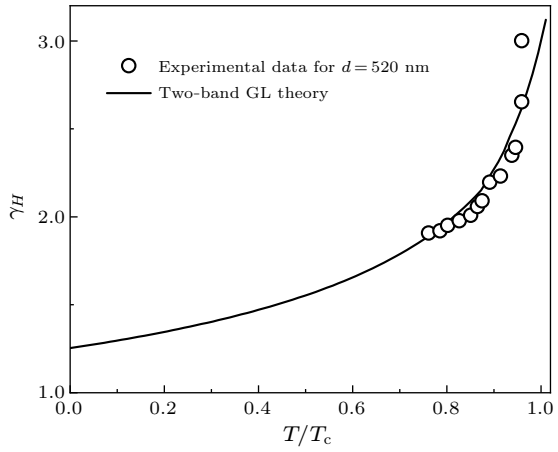


Fig. 4. The anisotropy parameter of the upper critical fields as a function of temperature for the FeSe film. The experimental data of the 520 nm-thick FeSe film with length 750 μm and width 150 μm are taken from Ref. [31].

In this stage, we can also define an anisotropy parameter for the upper critical fields $\gamma_H = H_{c2}^{\perp}/H_{c2}^{\parallel}$ and plot it as a function of temperature in Fig. 4. From Fig. 4, we can see that γ_H decreases with the decreasing temperature and our calculations are in accordance with the experimental data. Since temperature-independent behavior of γ_H is expected for single-band superconductors, this temperature dependence is a manifestation of multi-band superconductivity.[42] All of our theoretical results thus strongly suggest the two-gap s-wave superconductivity in this material.

It is worth noting that from the fitting of our numerical data the band with the larger gap corresponds to the larger effective mass, and the ratio of effective masses between these two bands equals 6.2, which is consistent with the effective mass anisotropy $\eta_m = 5.7$ from the measurement of the angle-resolved photoemission spectroscopy.[43,44]

4. The in-plane critical supercurrent

Now let us investigate the uniform critical supercurrent density j_c through the FeSe film. We would like to declare that there is no external magnetic field applied to the layered system in this circumstance. We can suppose the supercurrent in the x-direction and take the solution of the two-band GL theory with the form $\Delta_\gamma(x) = |\Delta_\gamma| e^{i\phi_\gamma(x)}$. To minimize the interaction free energy density in Eq. (3), we have $\phi_1(x) = \phi_2(x)$ for $\varepsilon_{12} > 0$ or $\phi_1(x) = \phi_2(x) + \pi$ for $\varepsilon_{12} < 0$. In either case, we can define the supercurrent velocity $v_\gamma = \frac{\hbar}{m_\gamma}\frac{d\phi_\gamma}{dx}$ for each band and have the same relation $v_2/v_1 = \eta_m$.

We can easily rewrite the GL free energy Eq. (1) with the form of Δ_γ following the standard procedure[45]

$$\frac{F}{d} = \sum_\gamma \Big(-\alpha_\gamma |\Delta_\gamma|^2 + \frac{1}{2} m_\gamma v_\gamma^2 |\Delta_\gamma|^2 + \frac{\beta}{2}|\Delta_\gamma|^4 - 2|\varepsilon_{12}| \cdot |\Delta_1| \cdot |\Delta_2| \Big). \tag{15}$$

Then, for the fixed v_s we can minimize Eq. (15) with $|\Delta_\gamma|$ and find the optimum value of $|\Delta_\gamma|$ satisfying

$$D_1|\Delta_1| + \beta|\Delta_1|^3 - |\varepsilon_{12}| \cdot |\Delta_2| = 0, \tag{16}$$

$$D_2|\Delta_2| + \beta|\Delta_2|^3 - |\varepsilon_{12}| \cdot |\Delta_1| = 0, \tag{17}$$

where $D_\gamma(T) = m_\gamma v_\gamma^2/2 - \alpha_\gamma$. We can solve Eqs. (16) and (17) to the cubic order of $|\Delta_\gamma|$ and obtain

$$|\Delta_1|^2 = \frac{\varepsilon_{12}^4 - \varepsilon_{12}^2 D_1 D_2}{\beta(\varepsilon_{12}^2 D_2 + D_1^3)}, \quad |\Delta_2|^2 = \frac{\varepsilon_{12}^4 - \varepsilon_{12}^2 D_1 D_2}{\beta(\varepsilon_{12}^2 D_1 + D_2^3)}. \tag{18}$$

Similar to the single-band case,[45] we thus calculate the uniform supercurrent density from the two-band GL theory as

$$j(T) = 2e|\Delta_1|^2 v_1 + 2e|\Delta_2|^2 v_2 = \frac{2e}{\beta}\Big(\frac{\varepsilon_{12}^4 - \varepsilon_{12}^2 D_1 D_2}{\varepsilon_{12}^2 D_2 + D_1^3} v_1 + \frac{\varepsilon_{12}^4 - \varepsilon_{12}^2 D_1 D_2}{\varepsilon_{12}^2 D_1 + D_2^3} v_2 \Big). \tag{19}$$

With Eq. (19), we can apply the condition $\frac{dj(T)}{dv_1}\big|_{v_1 = v_{1c}} = 0$ to find the maximum $j(T)$, which is exactly the uniform critical

supercurrent density $j_c(T)$. It is easy to see from Eq. (19) that the ratio of critical supercurrent density $j_c(T)/j_c(0)$ is independent of β, and we plot our results in Fig. 5. From Fig. 5, we can see that our numerical calculations can fit the experimental measurements in a wide temperature range, and especially the positive curvature behavior near T_c, which generally indicates the multi-band character of the corresponding systems.

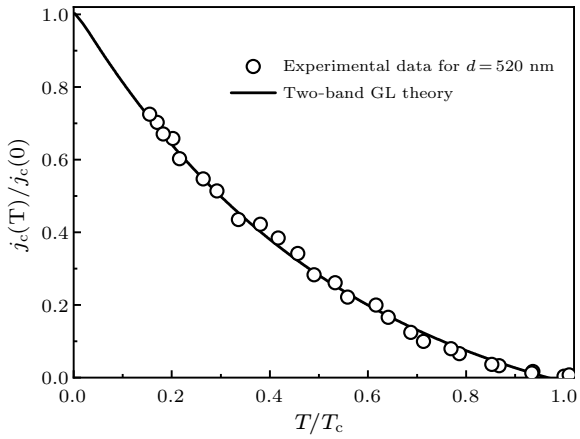


Fig. 5. Temperature dependence of critical supercurrent density for the FeSe film. The experimental data of the 520 nm-thick FeSe film with length 750 μm and width 150 μm are taken from Ref. [46].

5. Conclusion

In summary, based on the two-band GL theory we have investigated the temperature and angular dependence of the upper critical field in the FeSe thin film. It is found that the normalized upper critical field as a function of temperature is independent of the film thickness and our results are consistent with the experimental data. Furthermore, we also calculate the critical supercurrent density through the FeSe system which is also in accordance with the experimental measurements. Combining all of these facts, our theoretical work thus strongly suggests that the FeSe film is a two-gap s-wave superconductor. In addition, our mean-field analyses also show that the band with the larger gap corresponds to the one with the larger effective mass, and the ratio of the effective masses between these two bands is about 6.2. We hope that our theoretical results will inspire further research on better understanding the pairing symmetry and superconducting properties in iron-based materials.

Acknowledgment

It is a great pleasure to thank Professor H. Huang for patient guidance and helpful discussion.

References

[1] Kamihara Y, Watanabe T, Hirano M and Hosono H 2008 *J. Am. Chem. Soc.* **130** 3296
[2] Hsu F C, Luo J Y, Yeh K W, Chen T K, Huang T W, Wu P M, Lee Y C, Huang Y L, Chu Y Y, Yan D C and Wu M K 2008 *Proc. Natl. Acad. Sci. USA* **105** 14262
[3] McQueen T M, Huang Q, Ksenofontov V, Felser C, Xu Q, Zandbergen H, Hor Y S, Allred J, Williams A J, Qu D, Checkelsky J, Ong N P and Cava R J 2009 *Phys. Rev. B* **79** 014522
[4] Medvedev S, McQueen T M, Troyan I A, Palasyuk T, Eremets M I, Cava R J, Naghavi S, Casper F, Ksenofontov V, Wortmann G and Felser C 2009 *Nat. Mater.* **8** 630
[5] Imai T, Ahilan K, Ning F L, McQueen T M and Cava R J 2009 *Phys. Rev. Lett.* **102** 177005
[6] Sun J P, Matsuura K, Ye G Z, Mizukami Y, Shimozawa M, Matsubayashi K, Yamashita M, Watashige T, Kasahara S, Matsuda Y, Yan J Q, Sales B C, Uwatoko Y, Cheng J G and Shibauchi T 2016 *Nat. Commun.* **7** 12146
[7] Guo J G, Jin S F, Wang G, Wang S C, Zhu K X, Zhou T T, He M and Chen X L 2010 *Phys. Rev. B* **82** 180520
[8] Wang A F, Ying J J, Yan Y J, Liu R H, Luo X G, Li Z Y, Wang X F, Zhang M, Ye G J, Cheng P, Xiang Z J and Chen X H 2011 *Phys. Rev. B* **83** 060512
[9] Zhang Y, Yang L X, Xu M, Ye Z R, Chen F, He C, Xu H C, Jiang J, Xie B P, Ying J J, Wang X F, Chen X H, Hu J P, Matsunami M, Kimura S and Feng D L 2011 *Nat. Mater.* **10** 273
[10] Yan Y J, Zhang M, Wang A F, Ying J J, Li Z Y, Qin W, Luo X G, Li J Q, Hu J P and Chen X H 2012 *Sci. Rep.* **2** 212
[11] Ying T P, Chen X L, Wang G, Jin S F, Zhou T T, Lai X F, Zhang H and Wang W Y 2012 *Sci. Rep.* **2** 426
[12] Li W, Ding H, Deng P, Chang K, Song C L, He K, Wang L L, Ma X C, Hu J P, Chen X and Xue Q K 2012 *Nat. Phys.* **8** 126
[13] Sun L L, Chen X J, Guo J, Gao P W, Huang Q Z, Wang H D, Fang M H, Chen X L, Chen G F, Wu Q, Zhang C, Gu D C, Dong X L, Wang L, Yang K, Li A G, Dai X, Mao H K and Zhao Z X 2012 *Nature* **483** 67
[14] Dagotto E 2013 *Rev. Mod. Phys.* **85** 849
[15] Lu X F, Wang N Z, Wu H, Wu Y P, Zhao D, Zeng X Z, Luo X G, Wu T, Bao W, Zhang G H, Huang F Q, Huang Q Z and Chen X H 2015 *Nat. Mater.* **14** 325
[16] Lee J J, Schmitt F T, Moore R G, Johnston S, Cui Y T, Li W, Yi M, Liu Z K, Hashimoto M, Zhang Y, Lu D H, Devereaux T P, Lee D H and Shen Z X 2014 *Nature* **515** 245
[17] Peng R, Shen X P, Xie X, Xu H C, Tan S Y, Xia M, Zhang T, Cao H Y, Gong X G, Hu J P, Xie B P and Feng D L 2014 *Phys. Rev. Lett.* **112** 107001
[18] Peng R, Xu H C, Tan S Y, Cao H Y, Xia M, Shen X P, Huang Z C, Wen C H P, Song Q, Zhang T, Xie B P, Gong X G and Feng D L 2014 *Nat. Commun.* **5** 5044
[19] Wang M J, Luo J Y, Huang T W, Chang H H, Chen T K, Hsu F C, Wu C T, Wu P M, Chang A M and Wu M K 2009 *Phys. Rev. Lett.* **103** 117002
[20] Agatsuma A, Yamagishi T, Takeda S and Naito M 2010 *Physica C* **470** 1468
[21] Shen B, Feng Z P, Huang J W, Hu Y, Gao Q, Li C, Xu Y, Liu G D, Yu L, Zhao L, Jin K and Zhou X J 2017 *Chin. Phys. B* **26** 077402
[22] Schneider R, Zaitsev A G, Fuchs D and von Löhneysen H 2014 *J. Phys.: Condens. Matter* **26** 455701
[23] Farrar L S, Bristow M, Haghighirad A A, McCollam A, Bending S J and Coldea A I 2020 *npj Quantum Mater.* **5** 29
[24] Aichhorn M, Biermann S, Miyake T, Georges A and Imada M 2010 *Phys. Rev. B* **82** 064504
[25] Yamasaki A, Matsui Y, Imada S, Takase K, Azuma H, Muro T, Kato Y, Higashiya A, Sekiyama A, Suga S, Yabashi M, Tamasaku K, Ishikawa T, Terashima K, Kobori H, Sugimura A, Umeyama N, Sato H, Hara Y, Miyagawa N and Ikeda S I 2010 *Phys. Rev. B* **82** 184511
[26] Jiang K, Hu J P, Ding H and Wang Z Q 2016 *Phys. Rev. B* **93** 115138
[27] Zhou S, Kotliar G and Wang Z Q 2011 *Phys. Rev. B* **84** 140505
[28] Hu J P and Yuan J 2016 *Front. Phys.* **11** 117404
[29] Biswas P K, Salman Z, Song Q, Peng R, Zhang J, Shu L, Feng D L, Prokscha T and Morenzoni E 2018 *Phys. Rev. B* **97** 174509
[30] Sprau P O, Kostin A, Kreisel A, Böhmer A E, Taufour V, Canfield P C, Mukherjee S, Hirschfeld P J, Andersen B M and Séamus Davis J C 2017 *Science* **357** 75
[31] Schneider R, Zaitsev A G, Fuchs D and Hott R 2020 *Supercond. Sci. Technol.* **33** 075011
[32] Sun Y, Zhang W H, Xing Y, Li F S, Zhao Y F, Xia Z C, Wang L L, Ma X C, Xue Q K and Wang J 2014 *Sci. Rep.* **4** 6040
[33] Askerzade I N, Gencer A and Güclü N 2002 *Supercond. Sci. Technol.* **15** L13
[34] Gurevich A 2003 *Phys. Rev. B* **67** 184515
[35] Zhitomirsky M E and Dao V H 2004 *Phys. Rev. B* **69** 054508
[36] Liu M X and Gan Z Z 2007 *Chin. Phys. B* **16** 826

[37] Liu M X 2011 *Acta Phys. Sin.* **60** 017401 (in Chinese)
[38] Silaev M and Babaev E 2012 *Phys. Rev. B* **85** 134514
[39] Huang H, Lu Y Y and Wang W J 2012 *Acta Phys. Sin.* **61** 167401 (in Chinese)
[40] Liu M X, He L, Zhang G, Ye H, Huang X Y and Xu Y Z 2016 *Acta Phys. Sin.* **65** 037401 (in Chinese)
[41] Kong Y, Dolgov O V, Jepsen O and Andersen O K 2001 *Phys. Rev. B* **64** 020501
[42] Khim S, Lee B, Kim J W, Choi E S, Stewart G R and Kim K H 2011 *Phys. Rev. B* **84** 104502
[43] Watson M D, Kim T K, Haghighirad A A, Davies N R, McCollam A, Narayanan A, Blake S F, Chen Y L, Ghannadzadeh S, Schofield A J, Hoesch M, Meingast C, Wolf T and Coldea A I 2015 *Phys. Rev. B* **91** 155106
[44] Rhodes L C, Eschrig M, Kim T K and Watson M D 2022 *Front. Phys.* **10** 859017
[45] Tinkham M 1996 *Introduction to Superconductivity*, 2nd Edn. (New York: McGraw-Hill)
[46] Schneider R, Zaitsev A G, Fuchs D and Hott R 2019 *Supercond. Sci. Technol.* **32** 025001